Available online at www.sciencedirect.com
ScienceDirect
Earth and Planetary Science Letters 255 (2007) 306–323
EPSL
www.elsevier.com/locate/epsl

Age and duration of the Emeishan flood volcanism, SW China: Geochemistry and SHRIMP zircon U–Pb dating of silicic ignimbrites, post-volcanic Xuanwei Formation and clay tuff at the Chaotian section

Bin He [a], Yi-Gang Xu [a,*], Xiao-Long Huang [a], Zhen-Yu Luo [a], Yu-Ruo Shi [b], Qi-Jun Yang [a], Song-Yue Yu [a]

[a] *Key Laboratory of Isotope Geochronology and Geochemistry, Guangzhou Institute of Geochemistry, Chinese Academy of Science, Guangzhou, 510640, China*
[b] *Institute of Geology, Chinese Academy of Geological Sciences, Beijing 100037, China*

Received 3 August 2006; received in revised form 21 December 2006; accepted 22 December 2006
Available online 4 January 2007
Editor: R.W. Carlson

Abstract

The age and duration of the Emeishan basalts (SW China) remain poorly constrained largely due to the severe thermo-tectonic overprinting of the Ar–Ar system and failure to obtain zircon separates from erupted basalts. In an attempt to solve this problem, geochemical analyses and SHRIMP zircon U–Pb dating have been carried out on rare felsic ignimbrite in the uppermost of the Emeishan lava succession, the Xuanwei Formation which immediately overlies the Emeishan basalts and a clay tuff at the Middle–Late Permian boundary at the Chaotian section. Clastic rocks of the lowermost Xuanwei Formation (Group 1) in eastern Emeishan large igneous province (LIP) have a geochemical affinity to the Emeishan felsic volcanic rocks, whereas the overlying sediments (Group 2) are compositionally more akin to mafic components of the Emeishan traps. This is the reverse of volcanic sequence of the central Emeishan LIP where the felsic extrusives sit above predominant mafic rocks. It is likely that the clastic rocks are water-transported sediments resulting from erosion of the volcanic rocks in the center of the Emeishan LIP. This interpretation is further supported by the general agreement between the age of the lowermost Xuanwei Formation (257±4 Ma; 260±5 Ma) and that of the silicic ignimbrite (263±4 Ma) and the clay tuff at the Middle–Late Permian boundary at Chaotian (260±5 Ma). These ages, interpreted as the termination age of the Emeishan volcanism, are indistinguishable within error from the Middle–Late Permian boundary age (260.4±0.4 Ma) and the main stage (259–262±3 Ma) of the Emeishan volcanism inferred from dating of mafic and alkaline intrusions in the Emeishan LIP. All these suggest that the emplacement of the Emeishan volcanism took place over a very short interval. Moreover, the temporal link and geochemical analyses suggest that the Chaotian clay at the Middle–Late Permian boundary was genetically related to the Emeishan silicic volcanism. This, together with the fact at that both the Emeishan basalts and the Chaotian clay rest on the Maokou Formation, leads us to infer that the Emeishan basalt was emplaced at the Middle–Late Permian boundary. In this sense, the Emeishan volcanism can be regarded as

* Corresponding author.
E-mail address: yigangxu@gig.ac.cn (Y.-G. Xu).

doi:10.1016/j.epsl.2006.12.021

a boundary event and its age is presumed at ~ 260 Ma. Although more precise dating is required, both stratigraphic correlation and chronologic data presented in this paper lend supports to the notion that the Emeishan volcanism was one of likely causes of the end-Guadalupian mass extinction.

Keywords: SHRIMP dating; age and duration; Xuanwei Formation; silicic ignimbrite; clay tuff; Emeishan flood volcanism; end-Guadalupian mass extinction

1. Introduction

Voluminous flood volcanism is potentially responsible for global climate change and mass extinction during geologic time [1–8]. A causative link has been considerably strengthened by the close temporal relationship between mass extinctions and large igneous provinces (LIPs) [2,7,9–12] and the extremely short eruption interval of flood volcanism that can overwhelm atmospheric and biospheric system [6]. The best example came from the Siberian traps, the largest subaerial volcanic event known on the Earth. Data suggest that formation of this massive province occurred at the Permian–Triassic boundary, coincident with the largest mass extinction event in geological history [9,10,12].

Another mass extinction event occurred at the Middle–Late Permian boundary, i.e., the end-Guadalupian event [13,14]. Courtillot et al. [4] and Hallam and Wignall [15] independently proposed that the end-Guadalupian mass extinction coincided with the eruption of the lavas that formed the Emeishan LIP in SW China. To test this proposition, a number of attempts have been made to establish the age and duration of the Emeishan flood volcanism [16–22]. Unfortunately, most of the $^{40}Ar/^{39}Ar$ radiometric dating yielded Mesozoic–Cenozoic overprint ages [18,21], which may be related to the Mesozoic and Cenozoic thermo-tectonic events in the western Yangtze Craton. Lo et al. [16] reported the main stage of mafic flood magmatism at ~ 251–253 Ma, and subordinate activity at ~ 255 Ma by using high-precision Ar–Ar dating on the volcanic and intrusive rocks of the Emeishan LIP. As a consequence, they argued for a temporal link with the Permian–Triassic boundary event. However this inferred main phase is not consistent with the fact that the Emeishan basalts are sandwiched by Middle Permian Maokou limestone and Late Permian Luopingian sediments. Such a stratigraphic correlation suggests that the Emeishan volcanism occurred during the early Late Permian [4] or at the Middle–Late Permian boundary. This discrepancy has been ascribed to problems associated with the calibration of the age of monitor standards [7].

So far, the most meaningful age for the Emeishan flood volcanism was provided by Sensitive High-Resolution Ion Microprobe (SHRIMP) U–Pb analyses of zircons separated from mafic and alkaline intrusions and dykes. Zhou et al. obtained a mean $^{206}U/^{238}Pb$ age of 259±3 Ma for zircons from the Xinjie sills, which were interpreted as part of the feeder system of the main mafic eruptive phase [17]. This age is identical within error to that of the Middle–Late Permian boundary, therefore in support of a temporal linkage with the end-Guadalupian biotic crisis. Similar zircon U–Pb age (261±4 Ma) has recently been obtained by Luo et al. [22] on the nepheline syenite from Maomaogou in central Emeishan LIP [22]. Guo et al. [20] obtained a slightly older age of 262±3 Ma on the zircons from dykes that intruded Devonian strata in western Sichuan and they interpreted this age as the onset of the flood volcanism. While the consistency between these ages and stratigraphic correlations highlights the usefulness of U–Pb zircon dating techniques in establishing the temporal framework of the LIPs, to the exact timing and duration of the Emeishan volcanism remains uncertain. The main problem is that the geologic significance of the dated material is unclear and whether intrusions (i.e., mafic sills and dykes) represent single or multiple events during the flood volcanic episode.

Severe thermo-tectonic overprinting of the Ar–Ar system and failure to obtain zircon separates from erupted basalts renders direct dating of the Emeishan basalts impossible at this stage. For this reason, rare felsic member occurring in the uppermost Emeishan basalts, the Xuanwei Formation which immediately overlies the Emeishan basalts and a clay tuff at the Middle–Late Permian boundary at the Chaotian section have been targeted for geochemical and SHRIMP zircon U–Pb analyses. In particular, the Xuanwei Formation (with thickness of 78–286 m and an average of ~ 200 m) is distributed systematically around the elliptical, Chuandian paleosurface in the center of the Emeishan LIP (Fig. 1b) [23,24], which most likely

formed as a consequence of plume-induced domal uplift [23]. It is thus possible that the formation of the Xuanwei Formation was related to erosion of the Emeishan volcanic rocks in the center of the province due to uplift of the Chuandian paleosurface [e.g., 25,26]. If this is the case, examination of the Xuanwei

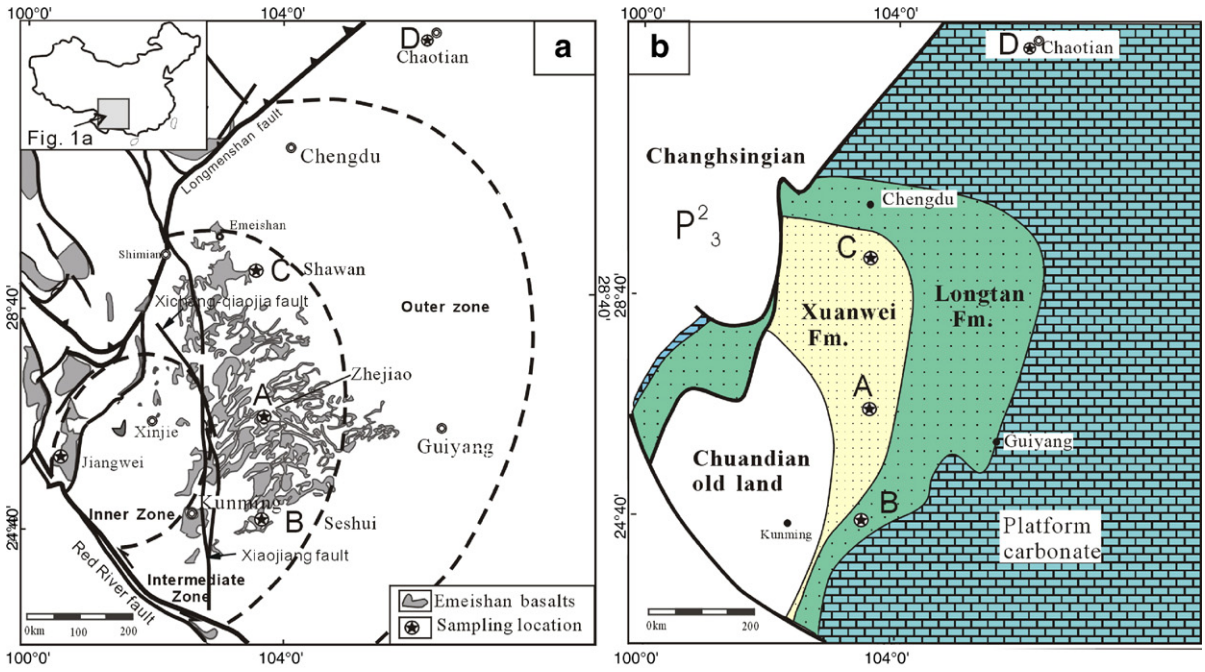

Formation could yield information about the pre-erosional lithologic components of the Emeishan volcanic rocks in the central LIP and eventually the timing of termination of the Emeishan flood volcanism. On the basis of geochemical evaluation, it will be shown that lowermost part of terrigenous Xuanwei sediments in the eastern Emeishan LIP were derived by erosion of the felsic member of the central Emeishan LIP. Consequently, the SHRIMP zircon U–Pb ages of the lowermost Xuanwei Formation and felsic member in uppermost Emeishan basalts provides constraints on the timing of termination of the Emeishan flood volcanism. This absolute age and relative temporal relationship, together with age (260.4±0.4 Ma) of the Middle–Late Permian boundary [27], has implications for the duration of Emeishan flood volcanism and relationships to the late Permian mass extinctions.

2. Geological background and sampling

The Emeishan LIP in SW China, which consists of massive flood basalts and numerous contemporaneous mafic and felsic intrusions, covers an area of more than 2.5×10^5 km^2 with a total thickness ranging from several hundred meters up to 5 km [28]. The relatively small exposure is most likely related to major disruption of the former igneous province along the Ailaoshan–Red River fault and the Longmenshan thrust belt [4,29] and subduction in the western Yangtze during closure of the paleoTethyan ocean [30]. The Emeishan flood volcanism succession comprises predominantly basaltic flows and pyroclastic deposits, with minor amounts of picrites and basaltic andesites. In addition, at Binchuan, where the thickest flood basalt is reported, several thin interbedded felsic layers form an important member in the uppermost sequence. So far, these felsic rocks are not documented in other places, probably due to intensive erosion in the central part of the LIP [23,24] (Fig. 1).

In the eastern LIP, the Emeishan basalts overlie the Middle Permian Maokou Formation, and are, in turn, overlain by the Late Permian Xuanwei (terrestrial clastic rocks) and Longtan (marine clastic rocks) Formations, which are of the Luopingian stage. The age of the top boundary of the Maokou Formation is roughly estimated at 258 Ma [25]. Therefore, stratigraphic data in the eastern LIP suggests that the Emeishan flood volcanism was erupted near the end-Guadalupian [4]. Recently, the age of Middle–Late Permian boundary is reported at 260.4±0.4 Ma [27] at Penglaitan, a global stratotype section and point (GSSP), which is located ca 400 km southeast from the Emeishan LIP. This provides a good reference from which the age of the Emeishan volcanism can be constrained. However, in most parts of the Emeishan LIP, the basalts overlie the Middle Permian Maokou Formation, but are overlain by Upper Triassic (e.g., the core of the LIP) or Lower Triassic (e.g., the west of the LIP) sedimentary rocks. Clearly, the relative time framework in the eastern LIP needs to be confirmed by radiometric dating which can provide absolute dates and the duration of the Emeishan volcanism.

Systematic stratigraphic studies and paleogeographic reconstructions reveal the presence of an elliptical, Chuandian paleosurface in the center of the Emeishan LIP (Fig. 1b) [23,24]. This paleosurface most likely formed as a consequence of plume-induced domal uplift and the accumulation of voluminous flood basalts and was maintained until the Late Triassic [23,24]. As indicated in Introduction, distribution of the Xuanwei Formation surrounding the Chuandian paleosurface suggests a possible genetic link between formation of the Xuanwei sediments and the erosion of the Emeishan volcanic rocks in the inner zone. Genesis of the Xuanwei Formation is therefore the key to define the pre-erosional lithologic components of the Emeishan volcanic rocks in the central LIP.

With these in the mind, top to bottom sampling of the Xuanwei Formation has been carried out at Zhejiao (Weining county, Guizhou province, Section A, Fig. 1), Seshui (Fuyuan county, Yunnan Province, Section B, Fig. 1) and Shawan (Emei county, Sichuan province, Section C, Fig. 1). In addition, clayey mudstones at the Middle–Late boundary at Chaotian (Guangyuan city, Sichuan Province) (Fig. 1) and a silicic ignimbrite in the uppermost part of Emeishan volcanic succession at Jiangwei (Eryuan county, Yunnan province) (Fig. 1) have also been sampled.

Fig. 1. (a) Schematic illustration of the geological features of the Emeishan large igneous province and the sampling locations; (b) lithofacies and paleogeography of the Late Permian (after the Emeishan volcanism) in the Upper Yangtze Craton; (c) stratigraphic sections the Xuanwei Formation and Early Triassic at four sampling localities in the eastern Emeishan Large igneous province. Section A — Zhejiao, Weining county, Guizhou province; Section B — Seshui, Fuyuan county, Yunnan province; Section C — Sawan, Emei county, Sichuan province; Section D — Chaotian, Guang'an county, Sichuan province. The numbers near the section indicate the thickness of the units. Dashed lines in (a) separate the inner, intermediate and the outer zones, which are defined in terms of extent of erosion of the Maokou Formation [23].

Table 1
Major element composition of the Xuanwei Formation sediments, ignimbrite in the upper sequence of the Emeishan volcanic succession and the clay layer from the Chaotian section (1)

	Group 1														Group 2		
Section	Zhejiao				Seshui						Shawan			Chaotian	Zhejiao		
Sample	ZJ-2	ZJ-3	ZJ-4	ZJ-5	SS-3	SS-4	SS-5	SS-6	SS-7	SS-8	SW-5	SW-6	SW-8	CT-2	ZJ-1	ZJ-6	ZJ-7
SiO_2	40.39	35.59	31.83	42.86	56.43	57.79	60.43	59.06	62.43	52.95	40.24	42.11	41.69	31.86	27.62	46.71	42.45
TiO_2	1.55	0.85	2.19	3.67	0.68	0.57	0.56	0.79	0.71	0.88	4.99	5.14	4.89	2.13	5.27	6.12	5.08
Al_2O_3	37.71	46.85	51.27	37.54	23.27	21.13	20.12	18.63	20.18	31.09	34.3	36.58	35.46	22.57	20.41	27.59	36.2
Fe_2O_3	6.42	1.86	1.42	0.63	7.18	8.09	7.61	8.1	5.86	2.2	6.58	2.62	4.4	3.9	33.64	6.72	2.17
MgO	0.11	0	0.21	0	0.37	0.17	0.21	0.54	0.55	0.51	0.16	0.13	0.22	0.43	3.3	0.22	0
CaO	0.03	0.06	0.04	0.08	0	<0.05	<0.05	<0.05	0.39	0.01	0.09	0.04	0.12	17.55	0.1	0.05	0.05
Na_2O	0.11	0.04	0.05	0.03	<0.1	<0.1	0.17	<0.1	<0.1	<0.1	0.4	0.13	0.14	<0.1	0	0	0
K_2O	0.05	0.67	0.77	0.15	2.17	0.54	0.65	2.14	2.2	2.24	0.1	0.03	0.04	0.47	0.17	0.68	0.14
MnO	0.01	0	0	0	0.04	0.09	0.04	0.06	0.04	0.03	0.02	0.01	0.03	0	0.12	0.01	0
P_2O_5	0	0.25	0.02	0.22	0.15	0.1	0.08	0.04	0.04	0.11	0.04	0.02	0.12	0.02	0.54	0.11	0.08
LOI	14.04	13.64	12.76	14.24	9.85	11.62	10.42	10.46	7.37	9.76	13.2	13.08	12.47	20.75	9.8	10.88	13.2
Total	100.42	100.05	100.55	99.42	100.15	100.1	100.31	99.82	99.75	99.79	100.13	99.88	99.56	99.68	100.97	99.09	99.37
KAT	24.39	55.05	23.44	10.24	34.03	37.06	35.67	23.54	28.52	35.21	6.87	7.11	7.25	10.59	3.87	4.51	7.13

$KAT = Al_2O_3/TiO_2$

Major element composition of the Xuanwei Formation sediments, ignimbrite in the upper sequence of the Emeishan volcanic succession and the clay layer from the Chaotian section (2)

	Group 2																
Section	Zhejiao																
Sample	ZJ-8	ZJ-9	ZJ-10	ZJ-11	ZJ-12	ZJ-13	ZJ-14	ZJ-15	ZJ-16	ZJ-17	ZJ-18	ZJ-19	ZJ-20	ZJ-21	ZJ-22	ZJ-23	ZJ-24	ZJ-25
SiO_2	52.86	22.79	45.28	43	61.44	46.8	53.46	39.33	51.22	46.03	45.63	49.92	48.83	55.58	47.07	48.62	55.85	53.32
TiO_2	3.4	1.95	4.51	5.11	3.09	6.26	4	5.03	3.37	5.32	3.06	6.09	5.8	5.2	6.32	6.21	3.83	4.72
Al_2O_3	15.63	10.82	20.85	23.78	13.35	31.06	21.3	22.16	14.68	23.71	15.17	25.43	28.46	25.08	27.72	30.81	25.37	22.19
Fe_2O_3	15.46	14.77	14.37	13.56	12.53	2.23	4.1	18.85	15.98	10.93	25.73	4.21	1.61	1.54	3.89	2.58	2.45	6.98
MgO	1.57	1.37	1.41	0.95	1.46	0.36	0.56	0.9	1.74	0.9	2.88	0.63	0.52	0.57	0.46	0.37	0.37	0.6

CaO	0.33	24.69	0.27	0.28	0.03	0.03	0.3	0.08	0.81	0.42	0.78	0.23	0.19	0.3	0.31	0.18	0.24	0.33
Na_2O	0	0.63	0	0	0	0	0.22	0	0.59	0	0.54	0	0	0	0.31	0	0.06	0.06
K_2O	0.89	0.24	1.25	1.1	0.7	0.46	1.17	0.63	0.67	0.84	0.07	0.86	0.93	1.5	0.48	0.97	1.34	1.68
MnO	0.07	1.06	0.13	0.01	0.05	0	0	0.03	0.1	0.02	0.07	0	0	0	0.01	0.01	0.03	0.02
P_2O_5	0.31	0.21	0.35	0.05	0.28	0.08	0.09	0.08	0.34	0.06	0.34	0.06	0.07	0.05	0.15	0.11	0.1	0.08
LOI	9.62	21.98	11.57	12.01	7.67	12.3	14.46	12.61	9.93	11.91	6.58	11.93	12.87	9.44	12.69	10.75	9.61	9.92
Total	100.13	100.5	99.99	99.86	100.61	99.58	99.66	99.7	99.43	100.16	100.86	99.35	99.27	99.28	99.4	100.61	99.26	99.9
KAT	4.6	5.54	4.63	4.65	4.32	4.96	5.33	4.4	4.36	4.45	4.96	4.18	4.91	4.82	4.39	4.96	6.62	4.7

$KAT = Al_2O_3/TiO_2$

Major element composition of the Xuanwei Formation sediments, ignimbrite in the upper sequence of the Emeishan volcanic succession and the clay layer from the Chaotian Section (3)

	Group 2																Ignimbrite
Section	Zhejiao			Seshui						Shawan							Jiangwei
Sample	ZJ-26	ZJ-29	ZJ-31	SS-1	SS-2	SS-9	SS-10	SS-11	SS-12	SW-1	SW-3	SW-4	SW-9	SW-14	SW-15	SW-16	JW-1
SiO_2	53.02	53.6	39.59	43.01	37.78	55.39	48.8	45.13	42.49	28.03	23.73	41.61	40.15	43.98	40.98	58.93	79.57
TiO_2	3	3.22	4.7	7.36	7.16	4.6	5.5	5.43	7.55	7.72	6.2	9.11	5.26	5.3	3.25	2.88	0.39
Al_2O_3	16.21	15.07	18.56	30.38	26.42	22.69	29.71	33.66	32.84	23.36	19.74	32.96	30.47	36.12	12.93	13.04	12.7
Fe_2O_3	13.94	13.49	24.37	6.91	12.11	3.77	5.12	3.41	3.38	27.32	39.09	3.55	11.12	0.62	13.46	9.9	2.37
MgO	4.37	4.61	1.69	0.32	0.18	0.89	0.32	0.22	0.19	0.79	0.35	0.21	0.23	0.08	3.44	4.36	0.21
CaO	2.63	2.51	0.04	<0.05	<0.05	0	0.03	0.04	0.05	1.63	1.47	0.16	0.16	0.09	11.66	2.41	0.12
Na_2O	2.83	3.77	0.04	<0.1	<0.1	<0.1	<0.1	<0.1	<0.1	<0.1	<0.1	<0.1	<0.1	<0.1	0.53	5.11	<0.1
K_2O	0.67	0.64	1.83	0.19	0.13	1.3	0.76	0.17	0.08	0.13	0.2	0.02	0.12	0.01	1.19	0.16	2.66
MnO	0.14	0.16	0.09	0.01	0	0.01	0.01	0.01	0.01	0.08	0.05	0.02	0.01	0.03	0.31	0.2	0
P_2O_5	0.35	0.28	0.53	0.06	0.07	0.08	0.11	0.09	0.09	1.04	0.93	0.13	0.08	0.06	0.27	0.24	0.01
LOI	2.38	3.17	9.35	12.05	15.86	10.91	9.77	12.18	12.38	10.11	7.95	12.28	12.53	13.13	12.47	2.48	2.43
Total	99.54	100.5	100.78	100.29	99.7	99.64	100.13	100.35	99.06	100.21	99.71	100.04	100.14	99.42	100.48	99.71	100.46
KAT	5.4	4.69	3.95	4.13	3.69	4.93	5.4	6.19	4.35	3.03	3.18	3.62	5.79	6.82	3.98	4.53	32.18

$KAT = Al_2O_3/TiO_2$.

3. Analytical methods

Sixty-seven samples were collected from the Xuanwei Formation and the Lower Triassic Feixianguan formation (Fig. 1) in the eastern Emeishan LIP, most of which are mudstones or clay rich rocks. Thin sections were made for each sample and examined under the microscope. Fifty-eight samples were analyzed for major element compositions at the Guangzhou Institute of Geochemistry, Chinese Academy of Sciences, using wave-length X-ray fluorescence spectrometry (XRF). Six of them were selected for ICP-MS analysis for their trace-element composition. Detailed descriptions of the analytical techniques are reported elsewhere [28].

Three mudstones (Sample ZJ-3, SW-1 and CT-2), which were collected from the lowermost unit of the Xuanwei Formation and one ignimbrite (Sample JW-1) in the uppermost Emeishan basalts at Jiangwei, Eryuan county, Yunnan province, were selected for U–Pb zircon dating. After chipping, 2 kg samples were ground to <0.1 mm in an agate mill. Zircons were separated using conventional heavy liquid and magnetic techniques and purified by hand-picking under a binocular microscope. Internal structure of the zircons was examined using cathodoluminescence (CL) imaging techniques prior to U–Pb isotopic analyses. The U–Pb analyses were performed using a Sensitive High-Resolution Ion Microprobe (SHRIMP II) at the Institute of Geology, Chinese Academy of Geological Sciences, Beijing. Detailed analytical procedures are similar to those described by Williams et al. [36]. The standard TEM zircons (417 Ma) were used in inter-element fractionation, and U, Th and Pb concentrations were determined based on the standard Sri Lankan gem zircon SL13 (572 Ma). Data processing was carried out using the SQUID 1.03 and Isoplot/Ex 2.49 programs of Ludwig [37,38], and the ^{204}Pb-based method of common Pb correction was applied. The reverse discordance in the U–Pb zircon concordia diagrams reflects relatively large uncertainties associated with ^{207}Pb/^{235}U ages, which may be related to correction of common lead that is difficult to determine precisely. However, this effect is minor for the ^{206}Pb/^{238}U ages. Consequently, the ages quoted in the text are ^{206}Pb/^{238}U ages, which are the weighted mean at the 95% confidence level.

4. Results

4.1. Rock description

Most samples of the Xuanwei Formation in three sections are mudstones or clay rich rocks, which have typical pelitic textures. However, some samples (e.g., ZJ-26 and ZJ-3) have relatively coarse grain size and can be classified as sandstones. Sample ZJ-26 mainly consists of basalt clasts, which are about 1–2 mm in size, well sorted and subrounded. Sample ZJ-3 also shows a clastic texture. Clasts in this sample are mostly light grey and subordinately black grey. They are rounded to angular in shape with size ranging from 1 to 4 mm. Some clasts show an irregular and tortured shape. Although sample ZJ-3 is strongly altered, tuffaceous and volcanic breccia textures flow-banding and vesicular structures are still preserved (see EPSL Online Supplement File A).

Sample JW-1 was taken from an interbedded felsic layer with a thickness of 6.5 m in the uppermost unit of the Emeishan basalt at Jiangwei, Eryuan county, Yunnan Province (Fig. 1). Its lithology mostly consists of ignimbrites, which are vitric tuffs with 60 to 80 vol.% glass and pumice, 15 to 30 vol.% free crystals, and 5 to 25 vol.% lithic fragments.

4.2. Major elements

Major element compositions of the samples collected from the Xuanwei and Feixianguan Formations are listed in Table 1. Loss on ignition (LOI) ranges from 8 to 22%, mostly around 12%. High LOI contents are consistent with a high percentage of clay minerals in these rocks. The analyses are characterized by high Al_2O_3 and Fe_2O_3 and low total alkali (K_2O+Na_2O) contents (0.01–2.56%), suggesting that these rocks were intensely weathered and altered. In particular, the samples collected from the bottom of the Xuanwei Formation (e.g., ZJ-1, SW-1, SW-3, SS-2) exhibit distinctively high content of Fe_2O_3 (33.64%–39.09%), Al_2O_3 (19.09–20.41%), TiO_2 (5.27–7.72%) and low SiO_2 (27.62–34.74%). These samples may represent strong alteration and weathering of the Emeishan flood basalts (Table 1).

For convenience, the sedimentary rocks of the Xuanwei Formation are divided into two groups in terms of Al_2O_3/TiO_2 ratio, a ratio that remains virtually constant during surficial weathering and alteration of rocks [30,31]. Group 1 samples have higher Al_2O_3/TiO_2 (7–55) than Group 2 samples (3.8 to 6.8). Fig. 2a shows the variation of the Al_2O_3/TiO_2 ratio with stratigraphic height for the Xuanwei and Feixianguan Formations at Zhaojiao, Weining county, western Guizhou province. This vertical distribution of Group 1 and Group 2 is also seen at Seshui (Fig. 2b) and Shawan Sections (Fig. 2c). The common feature of the compositional variation of the Xuanwei Formation at these three sections is that the

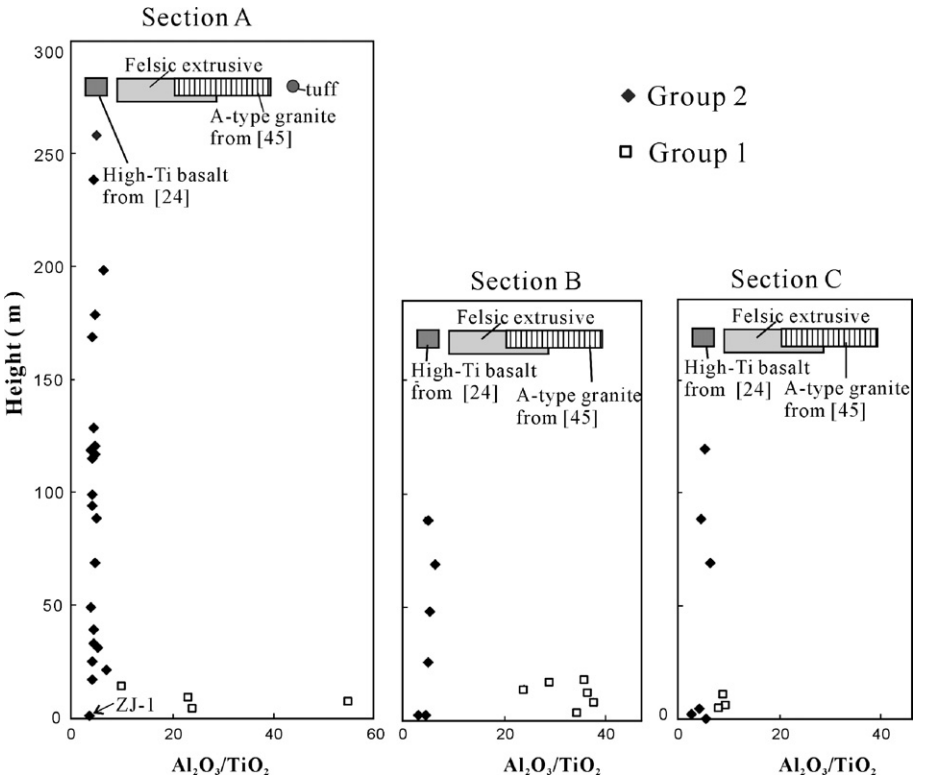

Fig. 2. Plot of Al_2O_3/TiO_2 ratio for the Xuanwei Formation sedimentary rocks against their stratigraphic height at three sections in eastern Emeishan LIP. Locations of sections are shown in Fig. 1. See text for the definition of Group 1 and Group 2 sediments. The range of Al_2O_3/TiO_2 ratio for high-Ti basalts is from Xu et al. [24]. The rhyolites and tuff were sampled from the center of the Emeishan large igneous province (unpublished data). The range of the Al_2O_3/TiO_2 ratio for A-type granites is from Zhang et al. [47].

Group 2 samples lie above the Group 1 samples (Figs. 1c and 2).

4.3. Trace elements

The Group 1 and Group 2 samples are also distinct in terms of their minor and trace element compositions. High field strength elements (HFSE) and contents in Group 1 samples (1141–4311 ppm) are much higher than those of Group 2 mudstones (302–966 ppm; Table 2). Rare earth elements (REE) contents in Group 1 samples are variable. ZJ-3 and ZJ-5 are much higher in total REE (2219 and 2648 ppm, respectively) than Group 2 mudstones (285–328 ppm; Table 2). However, REE contents in ZJ-2 and ZJ-4 are comparatively low (only 225 ppm and 20 ppm, respectively). Based on negative Eu anomaly, Group 1 could be further divided into two subgroups, i.e., Group 1a and Group 1b. REE patterns of Group 1a samples are strongly fractionated and possess strong negative Eu anomalies (Fig. 3a). The Group 1b sediments are characterized by weak negative Eu anomalies (Fig. 3b). In contrast, REE in Group 2 samples are less fractionated and show very weak to no Eu and positive anomalies (Fig. 3c). Fig. 3 also compares the REE patterns of the Xuanwei sediments with those of felsic and mafic rocks from the Emeishan LIP. The compositional similarity between Group 1 samples and rhyolites suggests a genetic link between them (Fig. 3a, b). On the other hand, the Group 2 samples compositionally resemble the Emeishan basalts, although more pronounced Sr anomalies are observed in sediments (Fig. 3c).

4.4. SHRIMP zircon U–Pb dating

4.4.1. Xuanwei Formation (ZJ-3 and SW-5)

ZJ-3 was collected from the lowermost unit of the Xuanwei Formation at Zhejiao, Weining county, Guizhou province, which directly overlies ~ 1000 m thick Emeishan basaltic sequence (Fig. 1c). Detrital zircons from this sample are clear, pale and euhedral. The well-developed tetragonal dipyramids in these crystals and oscillatory zoning (see EPSL Online

Table 2
Trace element concentration of the Xuanwei Formation sediments, ignimbrite in the upper sequence of the Emeishan volcanic succession and the clay layer from the Chaotian Section

	Group 1												Group 2						Ignimbrite
Section	Zhejiao				Seshui					Shawan		Chaotian	Zhejiao		Seshui	Shawan			Jiangwei
Sample	ZJ-2	ZJ-3	ZJ-4	ZJ-5	SS-3	SS-5	SS-6	SS-7	SS-8	SW-5	SW-8	CT-2	ZJ-8	ZJ-26	SS-1	SW-4	SW-9	SW-15	JW-1
Rb	1	20.9	4.1	7.2	43.7	13.3	49.4	45.9	58.4	6.6	1.7	15.7	34.8	11.3	7.5	1.4	6.6	39.5	115.5
Sr	4	156	3	120	122.4	35.4	43.4	33.3	90.7	36.6	207.6	79.5	31	201	60.2	150.7	46.4	130.9	63.7
Y	24	121	4	136	333	181.5	144.3	255	79.3	44.9	56.8	30.6	41	31	5.7	48.5	62.3	29.5	104.2
Zr	2783	828	1935	1858	3391	2804	2843	3349	832	1516	1519	506	367	294	326	807	674	239	1366
Nb	327	155	260	235	457.2	394	403.5	197.2	113.2	193.6	199.4	59.3	58	43	44.3	84	79.7	25.7	144.8
Ba	29.2	181.58	28.22	67	140.9	54	125	146.7	201.6	105.1	25.3	52.6	380.3	379.29	128.5	74.3	56.9	293.4	282.1
La	16.8	329.1	0.9	625.3	308.2	190.6	112.2	307.3	109.2	55.3	205.9	45.4	59.3	52.3	50	227.5	82	41.1	104.9
Ce	101	1005	4	1360	623.1	426.6	234.6	756.9	201.3	123.5	393.8	75.2	108	102	106.8	493.4	180.2	94.5	216.1
Pr	8	115	0	103	72	56.3	28.4	105.7	22.7	15.3	43.6	8.9	16	14	13.8	66.9	22.6	13.1	28.1
Nd	45	396	2	265	231.2	206.5	104.3	367.8	74.1	62.5	147.2	31.4	59	50	51.7	237	79.5	54.5	98.7
Sm	6.9	70.7	1.4	28.8	49.4	46.4	31.1	62.9	12.7	16.4	28.1	5.5	10.9	9.5	7.4	30.5	14.3	10.5	20
Eu	1	5.6	0.2	2.3	2.4	2.2	2	2.3	2.9	3.7	5.1	1.4	2.7	2.7	2.2	5.7	3.5	3.3	1.6
Gd	5.4	38.8	1.8	15.1	59.5	45.1	30.3	59.7	12.9	15.2	27.3	5.7	9.9	8	4.6	22.6	13.1	9.6	20.2
Tb	1.1	8.6	0.5	5.5	11.1	7.5	5.3	9.5	2.3	2	3.2	1	1.5	1.1	0.4	2.4	2	1.2	3.7
Dy	6.6	50.6	2.5	37.8	68.6	42.4	30.8	55.4	15	9.3	14	6	8.5	6.6	1.9	12.5	12.3	6.4	22.5
Ho	1.3	9.4	0.4	7.8	14	8.1	5.8	10.1	3.2	1.7	2.3	1.2	1.6	1.2	0.3	2.2	2.5	1.2	4.6
Er	3.6	26.1	0.9	24.6	38.7	21.7	15.9	27.3	9.9	4.3	6	3.5	4.1	3.2	0.8	6.6	7.3	3	13
Tm	0.6	4.7	0.1	4	5.8	3.1	2.4	3.5	1.4	0.6	0.7	0.5	0.6	0.5	0.1	0.9	1	0.4	1.9
Yb	3.8	33.4	1	28.5	34.3	20.2	15.1	20	9	4	4.7	3.2	3.5	2.7	0.9	5.4	6.3	2.3	12.2
Lu	0.51	4.13	0.12	3.87	5.1	3	2.2	2.7	1.4	0.6	0.7	0.5	0.53	0.4	0.1	0.8	0.9	0.3	1.8
Hf	63.79	27.72	40.59	44.35	93	73	71.1	82.7	20.1	34.6	37.4	13	10.54	7.87	8.1	20	16	5.4	33.2
Ta	22.13	9.57	17.15	16.59	37.1	29.9	28.8	30.4	7.8	12.7	13.5	4.3	4.16	3.02	3.3	5.9	5.7	1.7	10.9
Th	44.9	27	2.3	37.9	93.5	74.7	72.5	74.9	17.8	40	42	17.3	10.5	7.4	6.4	16.5	18.6	3.7	33.3
U	11.8	67.4	15.6	19.4	21.3	24.7	15	16.7	4.8	7.2	12.4	37.1	2.5	1.7	1.2	5.9	4.6	1	8.2
REE	226	2218	20	2648	1856	1261	765	2046	557	359	940	220	327	285	247	1163	490	271	654
HFSE	3220	1141	2257	2290	4311	3482	3491	3914	1053	1802	1826	613	481	379	387	966	838	302	1659

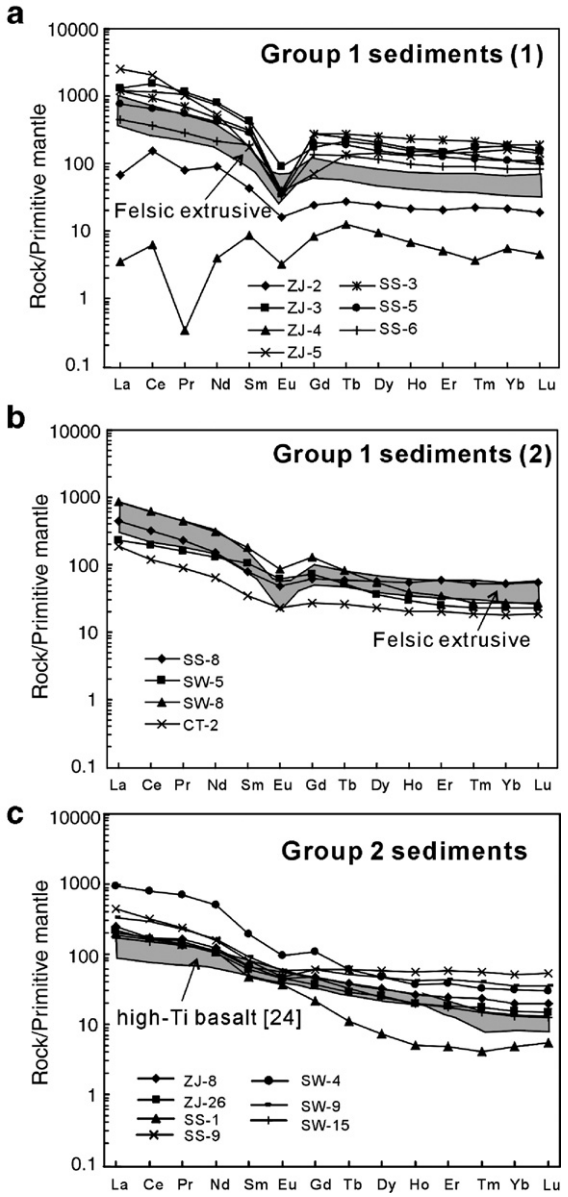

Fig. 3. Chondrite-normalized REE abundances (a, b, c) of Group 1 and Group 2 clastic rocks of the Xuanwei Formation. The compositions of mafic and felsic rocks of the Emeishan large igneous province [28,29] are shown for comparison. Normalization values are from [35].

Supplement File A) suggest an igneous origin. This is further confirmed by relatively high Th/U ratios of these zircons (~ 0.6) [39]. Zircon grains of sample ZJ-3 have a relatively wide range in U (81–577 ppm) and Th (45–364 ppm) concentrations. Among eighteen zircon grains analyzed, grain #8 yields a disconcordant age (~ 1100 Ma) (see EPSL Online Supplement File B). Although analysis of grain #7 was concordant, it yielded an age of 294 Ma which is significantly older than the majority of the analyses. These two grains are therefore excluded in age calculation. The remaining 16 zircon grains plot on the Concordia curve yielding a mean $^{238}U/^{206}Pb$ age of 257±4 Ma with a MSWD value of 2.2 (Fig. 4a and EPSL Online Supplement File B). This age represents the crystallization age of the source materials of the Xuanwei clastic sediments.

Sample SW-5 was collected from the lowermost part of the Xuanwei Formation at Shawan, Emei county, Sichuan province (Fig. 1a, b and Section C). Zircons analyses from this sample are very similar to those of sample ZJ-3, and the interpretation is identical. A total of 14 analyses from 14 zircons were made and most of them are concordant and near-concordant (Fig. 4b). A weighted mean $^{206}Pb/^{238}U$ age of 260±5 Ma with a MSWD value of 6.5 is interpreted as the crystallization age of the magmatic zircons.

4.4.2. Ignimbrite (JW-1)

JW-1 is a fine-grain ignimbrite collected from the uppermost part of the Emeishan basalts near Jiangwei (Eryuan county, Yunnan province). Zircons from this sample are clear, pale and euhedral. An igneous origin of these zircons is suggested based on the well-developed tetragonal dipyramids, oscillatory zoning and relatively high Th/U ratios of these zircons (~ 0.6). Thirteen analyses on 15 zircons form a cluster on the concordia plot (Fig. 4c) with a weighted mean $^{206}Pb/^{238}U$ age of 263±4 Ma with a MSWD value of 7.5. This is interpreted to represent the crystallization age of the magmatic zircons.

4.4.3. Clay at the Middle–Late Permian boundary (CT-02)

CT-2 is a clay collected at the Middle–Late Permian boundary at Chaotian. Zircon grains from this sample have a relatively wide range in U (52–641 ppm) and Th (29–295 ppm) concentrations. Th/U ratios of these zircons are rather constant (~ 0.6) except one (1.9). Among eighteen zircon grains analyzed, grain #6 yields a disconcordant age (~ 1250 Ma) (Table 3). Although analysis of grain #3 was concordant, it yields an age of 292 Ma which is significantly older than the majority of the analyses (EPSL Online Supplement File B). However, this age is close to 294 Ma observed in ZJ-3. Whether this 292–294 Ma age records a pre-Emeishan igneous activity in the region remains to assess. The remaining 16 zircon grains plot on the Concordia curve yielding a weighted mean $^{238}U/^{206}Pb$ age of 260±4 Ma with a MSWD value of 2.2 (Fig. 4d and EPSL Online

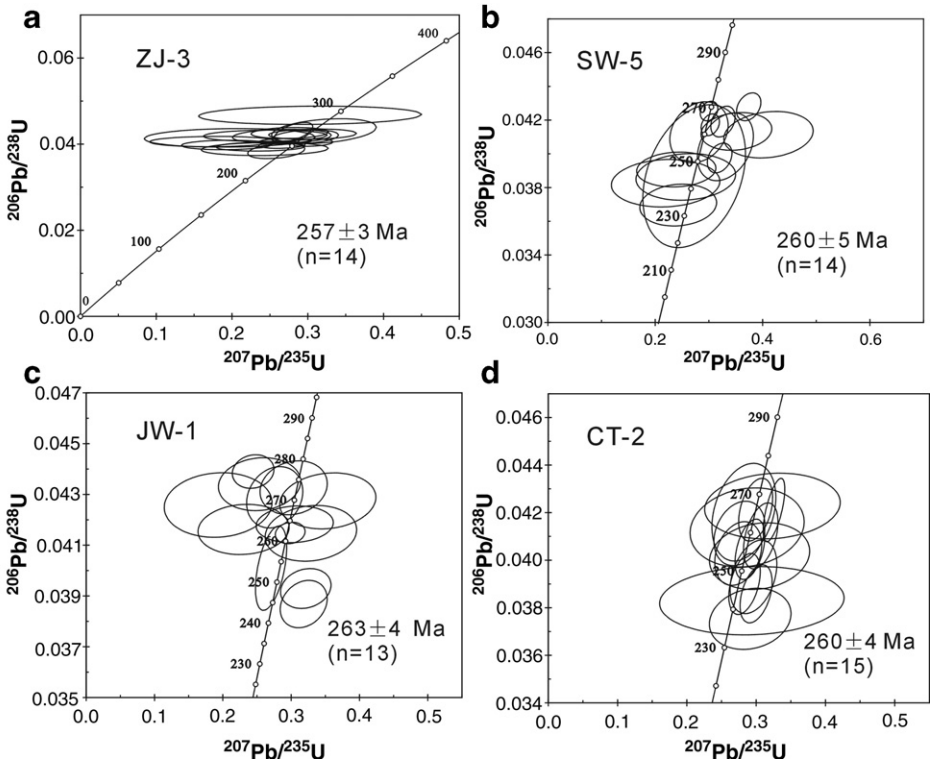

Fig. 4. SHRIMP U–Pb Concordia diagram of zircons from (a, b) the clastic sediments (ZJ-3, SW-5) from the lowermost Xuanwei Formation, (c) silicic ignimbrite (JW-1) in the uppermost of the Emeishan volcanic succession and (d) clayey tuff (CT-2) at the Middle–Late Permian boundary at Chaotian.

Supplement File B). This age represents the crystallization age of the source materials of felsic tuff.

5. Discussion

5.1. Provenance analysis of the Xuanwei Formation

As mentioned previously, the subcircular uplift, called as Chuandian "old land" in Chinese geologic literature [42], existed in the inner zone of the Emeishan LIP after the main period of Emeishan volcanism (Fig. 1b) and was maintained until the Late Triassic [23,24]. It is interesting to note that the distribution of the Xuanwei Formation (i.e., terrestrial clastic sediments of Upper Permian) is exclusively around this "old land". Moreover, the Xuanwei Formation is enclosed by marine clastic rocks of the Longtan Formation (Fig. 1b). Such a spatial configuration is strongly indicative of a genetic linkage between the uplift (and erosion) of the old land and the formation (and deposition) of the clastic rocks. It is possible that these clastic rocks of Late Permian were derived from the erosion of the uplifted old land during a tropical climate [28]. The gradual transition from the old land in the west, via terrigenous facies of the Xuanwei Formation to the marine facies of the Longtan Formation in the east reflects a paleosurface created by plume-induced doming [23].

In the Chuandian "old land", the Upper Triassic rocks directly cover the remnant Emeishan basalts, and therefore it is possible that the Xuanwei Formation may have been derived by weathering and transportation of the Emeishan basalts in the "old land" (i.e., in the center of the Province) [26]. The remnant in the inner zone of the Emeishan LIP indicates that the pre-erosional volcanic rocks are composed of mainly basalts and subordinate felsic rocks at the top of the lava succession [28,32]. These felsic rocks are therefore the most likely source for the lowermost unit (Group 1) of the Xuanwei Formation. This geological setting (i.e., terrestrial deposits and two possible source rocks) makes it possible to analyze the provenance of the Xuanwei Formation since the geochemical "fingerprints" of mafic and felsic extrusive rocks are very different.

The Al_2O_3/TiO_2 ratio is the most useful indicator of provenance [33,40]. For acidic tuff [26,40,43] it is typically >40, but ranges from 4 to 7 for mudstones

derived from mafic lavas [26,31]. The Al_2O_3/TiO_2 ratio of the Group 1 samples from the Xuanwei Formation at the Zhejiao section ranges from 7 to 55 (Table 1), which is comparable with the ratio (11–43) of the rhyolites and the tuff in the upper Emeishan LIP at Binchuan (unpublished data). Specifically, the Al_2O_3/TiO_2 ratio of sample ZJ-3 is as high as 55, a value typical of felsic volcanics [26,41]. This ratio is also similar to the Al_2O_3/TiO_2 ratio of the felsic tuff (42.7) in the upper Emeishan LIP at Binchuan (unpublished data). On the other hand, the Al_2O_3/TiO_2 ratio of the other 24 samples (Group 2) is significantly lower, ranging from 3.8 to 6.8, with an average of 5.5 (Table 1). This value is very similar to that of the Emeishan basalts (3.9–5.9) in the center of the province [28].

Trace element abundances and ratios of some immobile elements in the altered clastic rocks further assist with provenance analyses. The high field strength elements (HFSE), which are relatively immobile in the sedimentary environment, can be used to infer the source composition [34]. Because the HFSE are preferentially partitioned into melts during crystallization and anatexis, felsic rocks display an enrichment in HFSE in comparison to mafic rocks [40,44]. Higher HFSE abundances in the Group 1 sediments (1141–4311 ppm) compared to that of the Group 2 sediments (302–966 ppm) are consistent with the derivation of the former from the felsic rocks and the later from the mafic rocks.

REE compositions can also be used for monitoring the source composition because mafic rocks generally show less fractionated REE patterns with low LREE/HREE ratios and weak to no Eu anomalies. In contrast, felsic rocks usually show fractionated chondrite-normalized patterns and strong negative Eu anomalies [33,34]. Such characteristics can be preserved in sedimentary rocks [34,45,46]. The REE abundance in the Group 1 sediments (e.g. ZJ-3, ZJ-5, SS-3, 5, 6, 7, 8) is much higher than in the Group 2 samples (Table 2, Fig. 3). Moreover, the REE patterns of the Group 1a samples are strongly fractionated and possess strong negative Eu anomalies, resembling those of felsic extrusive in the uppermost Emeishan sequence and Late Permian A-type granites (co-magmatic with the Emeishan volcanism) in the center of the province [47]. The REE patterns of the Group 1b sediments possess weaker negative Eu anomalies, implying the involvement of the Emeishan basalt in the sedimentation processes. The low Al_2O_3/TiO_2 ratio of the Group 1b sediments (e.g., SW-5, 6.87; CT-2, 10.59) may have resulted from the mélange of mafic and felsic components. In contrast, REE in Group 2 samples are less fractionated and show weak to no Eu anomalies (Fig. 3c), a feature reminiscent of mafic rocks.

In summary, geochemical analysis suggests that the Group 1 sediments in the Xuanwei Formation exhibit a compositional affinity with felsic rocks though some samples (e.g., SW-5; CT-2) may mix with mafic composition, and the Group 2 samples are compositionally akin to mafic rocks. To gain further insights into the origin of the Xuanwei Formation, two additional Xuanwei sections at Seshui and Shawan (Fig. 1 and 2) have been examined. The results show that both Group 1 and Group 2 sediments are present at these localities (Tables 1, 2 and Fig. 2). Moreover, the stratigraphic correlation between the Group 1 and Group 2 sediments are the same at all three sections examined, that is, the Group 2 sediments sit above the Group 1 sediments (Fig. 2). This can therefore be taken as an intrinsic feature of the Xuanwei Formation.

If we consider the spatial distribution of the Xuanwei Formation exclusively surrounding the Chuandian old land (Fig. 1b), it is highly possible that the Group 1 sediments in the lowermost Xuanwei Formation were derived from the felsic members of the Emeishan LIP, and the Group 2 sediments from the mafic rocks (Fig. 5). A similar conclusion has been reached by Zhou et al. [31] who studied detrital claystones of the Xuanwei Formation. More importantly, the stratigraphic sequence of mafic-related Group 2 samples overlying the felsic-related Group 1 rocks in the Xuanwei Formation (Figs. 1 and 2) is the reverse of the volcanic sequence of the Emeishan lavas in which the rhyolites and trachytes occur above the basaltic lavas (Fig. 5). The Group 1 sediments have a thickness with a range of 2–20 m, some samples (e.g., ZJ-3) are typical of sandstones (EPSL Online Supplement File A). As a consequence, the formation of Group 1 sediments may have involved erosion and water transportation/deposition (Fig. 5). The Xuanwei Formation was formed after the termination of the Emeishan flood basalt volcanism. The uppermost silicic members in the center of the LIP were eroded first and the "felsic" materials were transported and deposited in the eastern LIP, forming the lowermost part of the Xuanwei Formation. Further erosion uncovered the mafic part of the Emeishan LIP and this eroded "mafic" material was deposited over those sediments derived from the felsic flows (Fig. 6). This interpretation finds its supporting evidence from the general agreement between the age of the lowermost Xuanwei Formation (257±4 Ma; 260±4 Ma) and that of the silicic ignimbrite in the uppermost of the Emeishan lava succession (263±5 Ma).

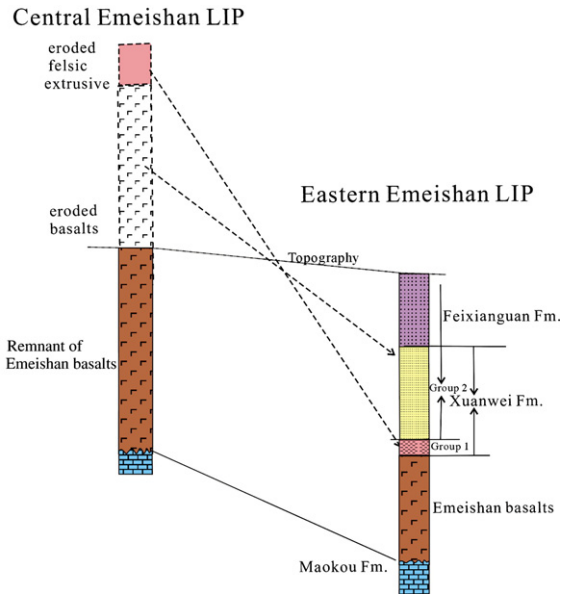

Fig. 5. Schematic illustration showing a possible origin of the Xuanwei Formation. Geochemically, Group 1 and Group 2 sediments of the Xuanwei Formation are related to the felsic and mafic components of the central Emeishan LIP, respectively. The stratigraphic sequence that the felsic-derived Group 1 and the mafic-derived Group 2 sediments is the reverse of the volcano-stratigraphy of the Emeishan volcanism where felsic extrusives post-dated mafic extrusives. It is likely that the Xuanwei sediments in the eastern Emeishan LIP resulted from unroofing, erosion and deposition of Emeishan volcanic rocks from the central LIP. Keys are the same as in Fig. 1.

5.2. Origin of the clay bed at the Middle–Late Permian boundary at Chaotian

A 2 m thick clay tuff bed between the Maokou Formation and Wujiaping Formation was recently documented at Chaotian (Northern Sichuan), ca 300 km north of the Emeishan LIP (Fig. 1a) [49]. Based on XRD, XRF and SEM analyses, Isozaki et al. [49] suggested that this clay bed originated from a volcanic ash of rhyolitic to dacitic composition, and proposed that a thick rhyo-dacitic ash bed must have covered most of South China at the end-Guadalupian. Isozaki et al. [49] argued that this felsic ash bed was not from the Emeishan LIP, mainly because of the dominant basaltic lava and pyroclastics in this LIP. Actually, the Emeishan LIP does have felsic extrusive in the uppermost unit of lava sequence [28,42,47]. Moreover, the above-mentioned provenance analyses and the widespread Xuanwei Formation strongly suggest that there was a significant felsic component in the Emeishan LIP, a feature shared by other continental LIP such as the Etendeka, Karoo and Yemen [50]. The volume of volcanic ash may imply either proximity to the source or unusually intense felsic volcanism. Given the genetic link and spatial proximity of the two events, the possible linkage between the Emeishan volcanism and the clay tuff bed between the Maokou and the Wujiaping Formations can be conceived.

To further elaborate this issue, we analyzed and dated a clayey mudstone sample (CT-2) collected at the Middle–Late Permian boundary at Chaotian. This sample is compositionally very similar to the silicic member of the Emeishan volcanism and the Group 1 sediments of the Xuanwei Formation (Tables 1 and 2). For instance, it exhibits a strongly fractionated REE pattern with a pronounced negative Eu anomaly. The Al_2O_3/TiO_2 ratio of CT-2 is 10.6, significantly higher than that of the mafic member (3.5–6.8) but close to that of felsic rocks (11.4–42.7). Moreover, SHRIMP U–Pb analyses on the zircons extracted from CT-2 yield a $^{238}U/^{206}Pb$ age of 260±4 Ma, which, despite its relatively large uncertainty, is virtually identical to the recommended age (260±0.4 Ma) of the Middle–late Permian boundary [23]. In addition, this age is indistinguishable within error from the age of the Emeishan silicic rocks (263±5 Ma) and from that (257±4 Ma; 260±4 Ma) of the lowermost Xuanwei Formation, whose precursor was the silicic members of the Emeishan volcanism. Therefore, both geochemical assessment and chronological data are consistent with the notion that the Emeishan volcanism was responsible for the clay tuff bed between the Maokou and the Wujiaping Formations (Fig. 6).

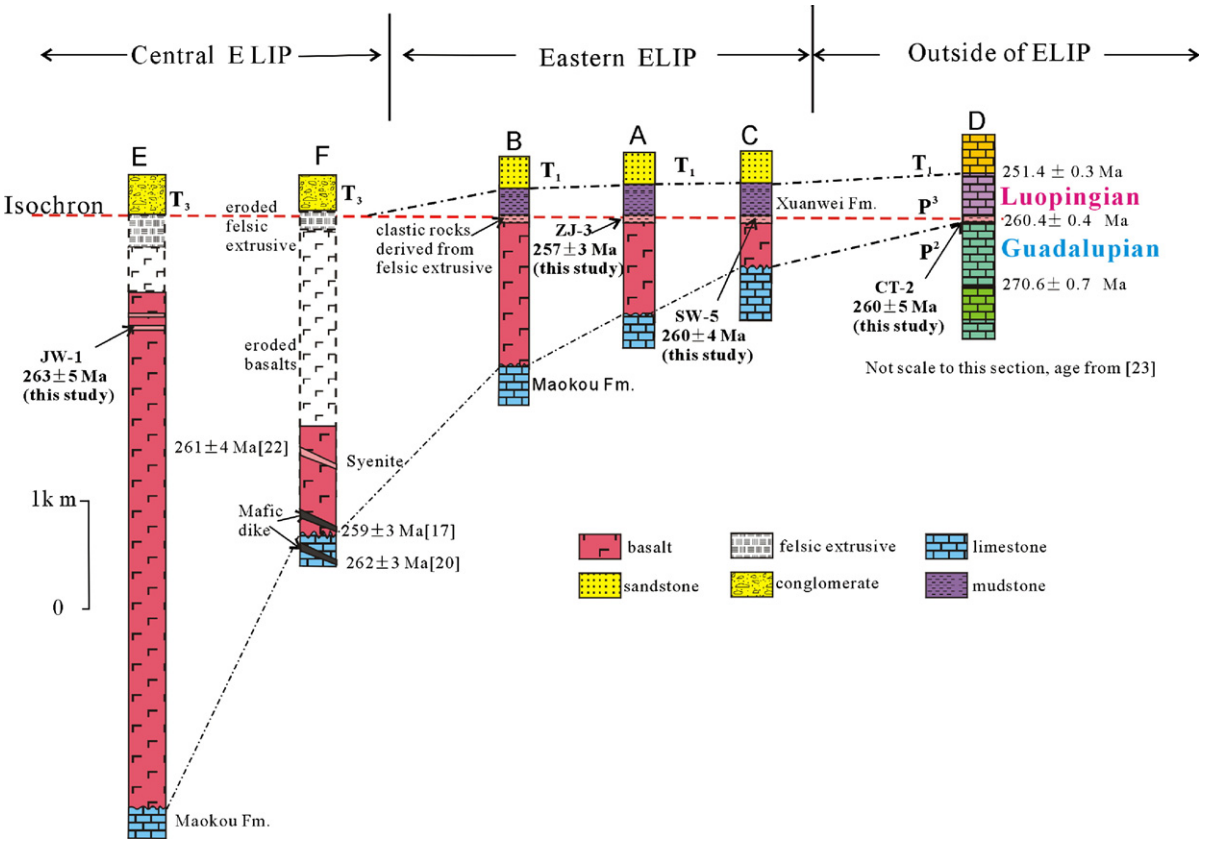

Fig. 6. Stratigraphic correlation in the Emeishan LIP and South China suggesting the emplacement of the Emeishan flood volcanism at the Middle–Late Permian boundary. Locations of sections A–D are shown in Fig. 1. Section E is a composite stratigraphic column at Binchuan; section F is a hypothetical stratigraphic column at Xinjie, central LIP, ages of mafic dikes are from [17,20], age of syenite from [22]. Erosion of volcanic rocks in this region provided materials to form the Xuanwei Formation. Ages of the P–Tr boundary, the base of the Changhsingian stage and the Middle–Late boundary of section D are from [51] and [27]. The thick dashed line marks the termination of the Emeishan flood volcanism. The dash-dot line indicates the onset of flood volcanism. These two lines join at Chaotian section imply that duration of the Emeishan flood volcanism is very short.

5.3. Emplacement of the Emeishan basalt at the Middle–Late Permian boundary

The Emeishan basalt is traditionally referred to as a lithological unit of the Upper Permian in China [42]. This notion is based on the initial definition of the Emeishan basalt Formation in the centre of the Emeishan LIP where the Emeishan basalts overlies the Middle Permian Maokou Formation and is overlain by Triassic sediments (Fig. 6 in [23]). It is this observation that led to the suggestion that the Emeishan basalts were mainly emplaced at the Permian–Triassic (P–Tr) boundary [16,24,32,48]. However it is now clear that the contact between the Triassic sequence and the Emeishan basalts is an erosional unconformity, which resulted from prolonged uplift of the central Emeishan LIP and concomitant erosion of the Emeishan basalts [23,24]. As a consequence the stratigraphic relationships in this region do not provide any unambiguous constraint on the timing of volcanism.

Courtillot and Renne [7] reviewed the ages of the major LIPs on Earth and put forward the hypothesis that most LIPs are emplaced in less than 1 Myr and linked them with major bioclimatic events. Based on this hypothesis, Courtillot et al. [4] predicted that the Emeishan LIP was emplaced at the end Guadalupian. This prediction finds supporting evidence in the eastern Emeishan LIP, where both Emeishan basalts and overlying strata (i.e., Late Permian Xuanwei and Longtan Formations) are not significantly eroded [23]. Lack of significant erosion of the Middle Permian Maokou Formation suggests that the onset of basaltic eruptions is close to the Middle–Late Permian boundary or at the end of the Guadalupian. A similar conclusion has been reached by He et al. [23] based on sedimentologic investigations of catastrophic deposits of the Middle Permian in the western Emeishan

LIP. Nevertheless, the stratigraphic constraint on the termination of Emeishan volcanism remains unclear, because it is not sure whether the Xuanwei Formation is a lateral equivalent of the Wuchiapingian or the Luopingian. For instance, if the Xuanwei Formation is only one of the constituent parts of the Late Permian, it follows that the Emeishan LIP was not necessarily emplaced *before* the Wuchiapingian stage. The data presented in this paper help clarify these ambiguities.

The petrogenetic assessment suggests that the sediments in the Xuanwei Formation were derived from the erosion of the Emeishan volcanic rocks in the inner zone. In particular, the Group 1 sediments in the lowermost of the Xuanwei Formation mainly represent eroded materials of the silicic member of the uppermost sequence of the Emeishan volcanic succession. Therefore the base of the Xuanwei Formation provides a firm limit on the termination of the Emeishan volcanism. On the other hand, the Chaotian clay bed is demonstrated to be genetically related to the Emeishan silicic volcanism. Therefore, felsic member in the uppermost Emeishan basalts, Group 1 sediments of Xuanwei Formation and clayey tuff at Late–Middle Permian boundary are located in an isochron horizon (Fig. 6). Given the fact that both the Emeishan basalts and the Chaotian clay rest on the Maokou Formation, it can be inferred, in particular, that the Emeishan basalt is the stratigraphic equivalent of the clay bed at the Chaotian section. It follows that the main phase of the Emeishan volcanism must have been emplaced *prior to* the Wuchiapingian stage and most likely occurred at the Middle–Late Permian boundary (Fig. 6).

5.4. Implication for age and duration of the Emeishan flood volcanism

The suggestion that the Emeishan volcanism is a boundary event yields important implications for the age of this large igneous province. Specifically, the age of the Middle–Late Permian boundary (260.4±0.4 Ma [27]) can be taken as the timing of the main phase of the Emeishan flood volcanism. This is consistent with the SHRIMP dates obtained on the Xinjie mafic intrusion (259±3 Ma). Zhou et al. [17] argued that the age of the Xinjie intrusion represents that of the main eruption of the Emeishan volcanism. Similar interpretation has been made by Kamo et al. [12] who showed that numerous mineralized intrusions are co-magmatic with the main phase of the Siberian basaltic volcanism [12].

The SHRIMP dates reported in this study provide further constraints on the age and duration of the Emeishan volcanism. JW-1 is a silicic ignimbrite in the uppermost part of the Emeishan as lava succession. Hence, the age of this sample (263±4 Ma) can be taken as the approximate estimate of the termination age of the Emeishan volcanism. Another independent constraint on the termination age of the Emeishan volcanism comes from the geochronologic data of the lowermost Xuanwei Formation which sits above the Emeishan basalts, because the Group 1 sediments, situated at the lowermost part of the Xuanwei Formation, may have resulted from deposition of eroded materials of the felsic extrusives (tuff or ignimbrite) of the Emeishan LIP. Since some of them are typical sandstone, it can be inferred that eroded materials were transported by water. This transportation and deposition is a natural process that concentrates zircon grains. The zircons in Group 1 sediments therefore inherited those of felsic extrusives. SHRIMP analyses on these zircons from two samples (ZJ-3, SW-5) yield 257±3 Ma and 260±5 Ma, respectively. The relatively large uncertainty could be due to detrital nature of the zircons in these samples. Nevertheless, these ages are identical within error to that of the silicic ignimbrite. Therefore diverse approaches yield consistent estimates on the termination age (~ 260 Ma) of the Emeishan volcanism.

It is important to note that the termination age of the Emeishan volcanism (257±4 Ma, 260±5 Ma, 263±5 Ma) is indistinguishable within error from the Middle–Late Permian boundary age (260.4±0.4 Ma) [27], and is also very close to the age of the main phase of volcanism (e.g., 259±3 Ma) [17] and ages (~ 260 Ma) of mafic and felsic intrusions in the Emeishan LIP [53–56]. Consequently, a very short duration can be inferred for the Emeishan volcanism although more precise dates are required in the future study. Previous arguments for a short duration of the Emeishan volcanism had been mainly based on the consideration of weathered features [28,52] and comparison of paleomagnetic data from a section in the east of the province with the perceived magnetostratigraphy of the period [57].

5.5. Implications for the end-Guadalupian mass extinction

Although Courtillot et al. [4] and Hallam and Wignall [15] independently proposed that the Emeishan volcanism may have been responsible for the end-Guadalupian mass extinction, the relation between these two events has not yet been fully explored [58]. Both stratigraphic and chronological data presented in this paper suggest that the Emeishan volcanism was emplaced at the Middle–Late Permian boundary, thereby providing new constraints on the temporal link between the Emeishan flood volcanism and the end-Guadalupian biotic crisis. It may be the rapidity of the

eruption that played a key factor in global climate and mass extinction in the Late Permian [6], although other causes such as severe sea level fall [15] should be evaluated as well in the future.

6. Conclusions

Based on geochemical analyses and SHRIMP zircon U–Pb dating of silicic ignimbrite in the uppermost Emeishan volcanic succession, clayey tuff at Middle–Late Permian boundary and clastic rocks of the Xuanwei Formation from three sections, the following conclusions can be drawn regarding the origin of the Xuanwei Formation and the timing of the Emeishan flood volcanism:

(1) Group 1 sediments in the lowermost part of Xuanwei Formation were genetically related to the felsic extrusive part of the Emeishan LIP, whereas the overlying Group 2 sediments were compositionally more akin to mafic part. This sedimentary sequence is the reverse of the Emeishan lava sequences in which rhyolites sit above the basaltic lavas, suggesting that the formation of the Xuanwei sediments was related to the unroofing, erosion and deposition of the Emeishan volcanic rocks in the center of the LIP. The widespread nature of the Xuanwei Formation in South China implies the existence of a significant felsic member in the uppermost part of the Emeishan LIP although felsic member was persevered in few localities. It is highly plausible that the Emeishan flood volcanism could have been responsible for the thick rhyolitic ash layer at the Middle–Late Permian boundary in South China. Therefore, felsic member in the uppermost Emeishan flood basalt, Group 1 sediments of Xuanwei Formation and the clayey tuff at Late–Middle Permian boundary are located on an isochron horizon, implying the emplacement of the Emeishan volcanism at the Middle–Late Permian boundary.

(2) SHRIMP zircon U–Pb dating of silicic ignimbrite in the uppermost Emeishan basalts, clay tuff at the Middle–Late Permian boundary at the Chaotian section and the lowermost clastic rocks of the Xuanwei Formation suggests that the Emeishan felsic extrusive rocks was erupted at ~ 260 Ma. Given that the felsic magmatism occurred in the uppermost lava succession, these dates are interpreted as the termination age of the Emeishan flood volcanism. This termination age is remarkably close to the estimated Middle–Late Permian boundary age and previous dating on mafic intrusions, implying a short duration of a few million years of volcanism. Both the temporal coincidence and the rapid eruption lend support to the conclusion that the Emeishan volcanism may be the cause of the end-Guadalupian mass extinction.

Acknowledgements

Drs. R. Ernst and MF Zhou are thanked for their careful and constructive reviews which substantially improved the paper. We gratefully acknowledge the financial supports from the National Natural Science Foundation of China (40421303; 40234046), the Chinese Academy of Sciences (the Bairen Project, KZCX2-101) and Guangzhou Institute of Geochemistry (A15-041107).

Appendix A. Supplementary data

Supplementary data associated with this article can be found, in the online version, at doi:10.1016/j.epsl.2006.12.021.

References

[1] W.J. Morgan, Flood basalts and mass extinctions, EOS Trans. AGU 67 (1986) 391.
[2] M.R. Rampino, R.B. Stothers, Flood basalt volcanism during the past 250 million years, Science 241 (1988) 663–668.
[3] V.E. Courtillot, Mass extinctions in the last 300 million years: one impact and seven flood basalts? Isr. J. Earth-Sci. 43 (1994) 255–266.
[4] V.E. Courtillot, C. Jaupart, I. Manighetti, P. Tapponnier, J. Besse, On causal links between flood basalts and continental breakup, Earth Planet. Sci. Lett. 166 (1999) 177–195.
[5] P.E. Olsen, Giant lava flows, mass extinctions, and mantle plumes, Science 284 (1999) 604–605.
[6] P.B. Wignall, Large igneous provinces and mass extinctions, Earth-Sci. Rev. 53 (2001) 1–33.
[7] V.E. Courtillot, P.R. Renne, On the age of flood basalt events, Geoscience 335 (2003) 113–140.
[8] J.P. Morgan, T.J. Reston, C.R. Ranero, Contemporaneous mass extinctions, continental flood basalts, and 'impact signals': are mantle plume-induced lithospheric gas explosions the causal link? Earth Planet. Sci. Lett. 217 (2004) 263–284.
[9] I.H. Campbell, G.K. Czamanske, V.A. Fedorenko, R.I. Hill, V. Stepanov, Synchronism of the Siberian traps and the Permian–Triassic boundary, Science 258 (1992) 1760–1763.
[10] P.R. Renne, Z.C. Zhang, M.A. Richards, M.T. Black, A.R. Basu, Synchrony and causal relations between Permian–Triassic boundary crises and the Siberian flood volcanism, Science 269 (1995) 1413–1416.
[11] C.J. Allegre, J.L. Brick, V.E. Courtillot, Age of Deccan traps using Re–Os systematics, Earth Planet. Sci. Lett. 170 (1999) 197–204.
[12] S.L. Kamo, G.K. Czamanske, Y. Amelin, V.A. Fedorenko, D.W. Davis, V.R. Trofimov, Rapid eruption of Siberian flood-volcanic rocks and evidence for coincidence with the Permian–Triassic

boundary and mass extinction at 251 Ma, Earth Planet. Sci. Lett. 214 (2003) 75–91.
[13] Y.G. Jin, J. Zhang, Q.H. Shang, Two phases of the end-Permian mass extinction. Pangea: global environments and resource, Can. Soc. Pet. Geol., Mem. 17 (1994) 813–822.
[14] S.M. Stanley, X. Yang, A double mass extinction at the end of the Paleozoic era, Science 266 (1994) 1340–1344.
[15] A. Hallam, P.B. Wignall, Mass extinction and sea-level changes, Earth-Sci. Rev. 48 (1999) 217–250.
[16] C.H. Lo, S.L. Chung, T.Y. Lee, G.Y. Wu, Age of the Emeishan flood magmatism and relations to Permian–Triassic boundary events, Earth Planet. Sci. Lett. 198 (2002) 449–458.
[17] M.F. Zhou, J. Malpas, X.Y. Song, P.T. Robinson, M. Sun, A.K. Kennedy, C.M. Lesher, R.R. Keays, A temporal link between the Emeishan large igneous province (SW China) and the end-Guadalupian mass extinction, Earth Planet. Sci. Lett. 196 (2002) 113–122.
[18] J.R. Ali, G.M. Thompson, M.F. Zhou, X.Y. Song, Emeishan Basalts Ar–Ar overprint ages define several tectonic events that affected the western Yangtze Platform in the Meso- and Cenozoic, J. Asian Earth Sci. 23 (2004) 163–178.
[19] W.M. Fan, Y.J. Wang, T.P. Peng, L.C. Miao, F. Guo, Ar–Ar and U–Pb chronology of late Paleozoic basalts in western Guangxi and its constraints on the eruption age of the Emeishan basalt magmatism, Chin. Sci. Bull. 49 (2004) 2318–2327.
[20] F. Guo, W.M. Fan, Y.J. Wang, C.W. Li, When did the Emeishan plume activity start? Geochronological evidence from ultramafic–mafic dikes in Southwestern China, Int. Geol. Rev. 46 (2004) 226–234.
[21] Z.Q. Hou, W. Chen, J.R. Lu, Collision events during 177–135 Ma on the eastern margin of the Qinghai–Tibet plateau: evidence from Ar-40/Ar-39 dating for basalts on the western margin of the Yangtze platform, Acta Geol. Sin. -Engl. Ed. 76 (2002) 194–204.
[22] Z.Y. Luo, Y.G. Xu, B. He, Y. Shi, X.L. Huang, Geochronologic and petrochemical evidence for the genetic link between the Maomaogou nepheline syenites and the Emeishan large igneous province, Chin. Sci. Bull. (in press).
[23] B. He, Y.G. Xu, S.L. Chung, L. Xiao, Y.M. Wang, Sedimentary evidence for a rapid, kilometer scale crustal doming prior to the eruption of the EFB, Earth Planet. Sci. Lett. 213 (2003) 391–405.
[24] Y.G. Xu, B. He, S.L. Chung, M.A. Menzies, F.A. Frey, The geologic, geochemical and geophysical consequences of plume involvement in the Emeishan flood basalt province, Geology 30 (2004) 917–920.
[25] Editing Committee of Stratigraphy, Permian in China, Geological Publishing House, Beijing, 2000 (Chinese with English abstract).
[26] Y.P. Zhou, Y.L. Ren, B.F. Bohor, Origin and distribution of tonsteins in Late Permian coal seams of southwestern China, Int. J. Coal Geol. 2 (1982) 49–77.
[27] F.M. Gradstein, J.G. Ogg, A.G. Smith, W. Bleeker, L.J. Lourens, A new geologic time scale, with special reference to PreCambrian and Neogene, Epoisodes 22 (2004) 83–99.
[28] Y.G. Xu, S.L. Chung, B.M. Jahn, G.Y. Wu, Petrologic and geochemical constraints on the petrogenesis of Permian–Triassic EFB in southwestern China, Lithos 58 (2001) 145–168.
[29] L. Xiao, Y.G. Xu, S.L. Chung, B. He, Chemostratigraphic correlation of Upper Permian lavas, Yunnan Province, China: extent of the Emeishan large igneous province, Int. Geol. Rev. 45 (2004) 753–766.
[30] F.T. Liu, J.H. Liu, J.K. He, Q.Y. You, The subducted slab of the Yangtze continental block beneath the Tethyan orogen in the western Yunnan, Chin. Sci. Bull. 45 (2000) 466–472.
[31] Y.P. Zhou, B.F. Bohor, Y.L. Ren, Trace element geochemistry of altered volcanic ash layers (tonsteins) in Late Permian coal-bearing formations of eastern Yunnan and western Guizhou Provinces, China, Int. J. Coal Geol. 44 (2000) 305–324.
[32] S.L. Chung, B.M. Jahn, G. Wu, C.H. Lo, B. Cong, The Emeishan flood basalt in SW China: a mantle plume initiation model and its connection with continental breakup and mass extinction at the Permian–Triassic boundary, in: M.J.F. Flower, S.L. Chung, C.H.L., T.Y. Lee (Eds.), Mantle Dynamics and Plate Interaction in East Asia, Geodynamics, vol. 27, 1998, pp. 47–58.
[33] R.L. Cullers, J. Graf, Rare earth elements in igneous rocks of the continental crust: intermediate and silicic rocks, ore petrogenesis, in: P. Henderson (Ed.), Rare-Earth Geochemistry, Elsevier, Amsterdam, 1983, pp. 275–312.
[34] S.R. Taylor, S.M. Mclennan, The Continental Crust: Its Composition and Evolution, Blackwell, Oxford, 1985.
[35] S.S. Sun, W.F. McDonough, Chemical and isotopic systematics of oceanic basalts: implications for mantle composition and processes, in: A.D. Saunders, M.J. Norry (Eds.), Magmatism in the Ocean Basins, Geol. Soc. London, Spec. Publ., vol. 42, 1989, pp. 313–345.
[36] I. Williams, U–Th–Pb geochronology by ion microprobe, in: M.A. McKibben, W.C. Shanks III, W.I. Ridley (Eds.), Applications of microanalytical techniques to understanding mineralizing processes, Rev. Econ. Geol., vol. 7, 1998, pp. 1–35.
[37] K.R. Ludwig, Squid 1.02, in A User Manual, Berkeley, Berkeley Geochronological Center Special Publication, 2001, pp. 1–219.
[38] K.R. Ludwig, Using Isoplot/EX, version 2.49, A Geolocronolgical Toolkit for Microsoft Excel, Berkeley, Berkeley Geochronological Center Special Publication, 2001, pp. 1–55.
[39] P.W.O. Hoskin, U. Schaltegger, The composition of zircon and igneous and metamorphic petrogenesis, in: J.M. Hanchar, P.W.O. Hoskin (Eds.), Zircon, Reviews in Mineralogy and Geochemistry, vol. 53, 2003, pp. 27–55.
[40] J.M.G. Lopez, B. Bauluz, C.F. Nieto, A.Y. Oliete, Factors controlling the trace-element distribution in fine-grained rocks: the Albian kaolinite-rich deposits of the Oliete Basin (NE Spain), Chem. Geol. 214 (2005) 1–19.
[41] L. Zhou, F.T. Kyte, The Permian–Triassic boundary event: a geochemical study of three Chinese sections, Earth Planet. Sci. Lett. 90 (1988) 411–421.
[42] Bureau of geology and mineral resources of Sichuan province, Regional geology of Sichuan province, Geological Publishing House, Beijing, 1991 (in Chinese with English abstract).
[43] D.A. Spears, R. Kanaris-Sotiriou, A geochemical and mineralogical investigation of some British and other European tonsteins, Sedimentology 26 (1979) 407–425.
[44] R. Feng, R. Kerrich, Geochemistry of fine-grained clastic sediments in the Archean Abititi greenstones belt, Canada: implication for province and tectonic setting, Geochim. Cosmochim. Acta 54 (1990) 1061–1081.
[45] D.J. Wronkiewicz, K.C. Condie, Geochemistry of Archean shales from the Witwatersrand and from Fig Tree Group, South Africa, Geochim. Cosmochim. Acta 37 (1987) 2401–2416.
[46] R.L. Cullers, V.N. Podkovyrov, The source and origin of terrigenous sedimentary rocks in the Mesoproterozoic Ui Group, southeastern Russia, Precambrian Res. 117 (2002) 157–183.
[47] Y.X. Zhang, Y.N. Luo, Z.X. Yang, Panxi Rift, Geological Publishing House, Beijing, 1988 (in Chinese with English abstract).

[48] S.L. Chung, B.M. Jahn, Plume–lithosphere interaction in generation of the EFB at the Permian–Triassic boundary, Geology 23 (1995) 889–892.
[49] Y. Isozaki, J.X. Yao, T. Matsuda, H. Sakai, Z.S. Ji, N. Shimizu, N. Kobayashi, H. Kawahata, H. Nishi, M. Takano, T. Kubo, Stratigraphy of the Middle–Upper Permian and Lower Triassic at Chaotian, Sichuan, China, Proc. Jpn. Acad., Ser. B Phys. Biol. Sci. 80 (2004) 10–16.
[50] S.E. Bryan, T.R. Rilly, D.A. Jerram, C.J. Stephens, P.T. Leat, Silicic volcanism: an undervalued component of large igneous provinces and volcanic rifted margins, in: M.A. Menzies, S.L. Klemperer, C.J. Ebinger, J. Baker (Eds.), Geological Society of American Special Paper, vol. 362, Volcanic Rifted Margins, Boulder, Colorado, 2002, pp. 97–118.
[51] S.A. Bowring, D.H. Erwin, Y.G. Jin, M.W. Martin, E. Davidek, W. Wang, U/Pb zircon geochronology and tempo of the end-Permian mass extinction, Science 280 (1998) 1039–1045.
[52] G.M. Thompson, J.R. Ali, X.Y. Song, D.W. Jolley, Emeishan basalts, southwest China: reappraisal of the formation's type area stratigraphy and a discussion of its significance as a LIP, J. Geol. Soc. (Lond.) 158 (2001) 593–599.
[53] M.-F. Zhou, P.T. Robinson, C.M. Lesher, R.R. Keays, C.-J. Zhang, J. Malpas, Geochemistry, petrogenesis, and metallogenesis of the Panzhihua gabbroic layered intrusion and associated Fe–Ti–V–oxide deposits, Sichuan Province, SW China, J. Petrol. 46 (2005) 2253–2280.
[54] M.F. Zhou, J.H. Zhao, L. Qi, W. Su, R.Z. Hu, Zircon U–Pb geochronology and elemental and Sr–Nd isotopic geochemistry of Permian mafic rocks in the Funing area, SW China, Contrib. Mineral. Petrol. 151 (2006) 1–19.
[55] H. Zhong, W.G. Zhu, Geochronology of layered mafic intrusions from the Pan–Xi area in the Emeishan large igneous province, SW China, Miner. Depos. 41 (2006) 599–606.
[56] H. Zhong, W.G. Zhu, Z.Y. Chu, D.F. He, X.Y. Song, Shrimp U–Pb zircon geochronology, geochemistry, and Nd–Sr isotopic study of contrasting granites in the Emeishan large igneous province, SW China, Chem. Geol. 236 (2007) 112–133.
[57] K.N. Huang, N.D. Opdyke, Magnetostratigraphic investigations of an Emeishan basalt section in western Guizhou Province, China, Earth Planet. Sci. Lett. 163 (1998) 1–14.
[58] J.R. Ali, G.M. Thompson, M.F. Zhou, X.Y. Song, Emeishan large igneous province, SW China, Lithos 79 (2005) 475–489.